Polymer Testing 31 (2012) 971–977

Contents lists available at SciVerse ScienceDirect

Polymer Testing

journal homepage: www.elsevier.com/locate/polytest

Material properties

Polypyrrole nanoparticles coated amorphous short silica fibers: Synthesis and characterization

Claudia Merlini*, Bruna S. Rosa, Daliana Müller, Luiz G. Ecco, Sílvia D.A.S. Ramôa, Guilherme M.O. Barra*

Polymer and Composites Laboratory, Mechanical Engineering Department, Federal University of Santa Catarina – UFSC, Campus Universitário, 88040-900 Florianópolis, Santa Catarina, Brazil

ARTICLE INFO

Article history:
Received 23 May 2012
Accepted 4 July 2012

Keywords:
Polypyrrole
Amorphous silica short fibers
Poly(styrene-b-ethylene-ran-buthylene-b-styrene) copolymer
Conductive filler

ABSTRACT

Polypyrrole-coated amorphous silica short fibers (PPy-ASF) were obtained through *in situ* oxidative polymerization of pyrrole (Py) on the ASF surface by using ferric chloride ($FeCl_3$) as oxidant. These conducting fibers were constituted of PPy particles packed close together to form a continuous conductive layer on the ASF surface which was responsible for electrical conductivity of 0.32 $S.cm^{-1}$, similar to that found for pure PPy. The PPy-ASF were blended with polystyrene-block-poly(ethylene-ran-butylene)-block-polystyrene copolymer (SEBS) through solution casting at room temperature to form conductive rubbery (SEBS/PPy-ASF) composites. The electrical conductivity and percolation threshold of SEBS/PPy-ASF films were evaluated and also compared with PPy filled SEBS blends (SEBS/PPy) prepared under the same processing conditions. SEBS/PPy-ASF displayed lower percolation threshold and higher electrical conductivity values than those found for SEBS/PPy blends at the same conductive filler concentration. The high PPy-ASF aspect ratio (length to diameter ratio, L:D) and their good electrical conductivity allow production of conductive polymer composites at very low percolation threshold. The results obtained in this study reveal that PPy-ASF materials are promising candidates to be used as conductive filler for developing conducting polymer composites.

1. Introduction

For over three decades, intrinsically conducting polymers (ICP's) have been extensively studied because of their interesting properties for a number of applications, including solar cells, sensors, electromagnetic shielding paint, electrochromic devices, light weight rechargeable batteries, neural probes, drug-delivery devices and scaffold for tissue engineering [1–5]. Polypyrrole (PPy) is a promising ICP due to its environmental stability, ease of synthesis and electrical conductivity that can be controlled by changing the doping degree. However, its use in commercial applications has been hampered because of the poor processability and inadequate mechanical properties. Several techniques have been studied in the literature to overcome these problems [5–7].

Methods based on the dispersion of polypyrrole in an insulating polymer matrix have been reported to be quite efficient due to the possibility of combining the rheological and mechanical properties of the polymer matrix with the ICP properties. These materials are normally characterized by an insulator-conductor transition at an appropriate conducting polymer weight or volume fraction, known as the percolation threshold point. Low percolation threshold is required to minimize processing problems and depletion of the mechanical performance of the host polymer. The properties and percolation threshold of conducting

* Corresponding authors.
E-mail addresses: claudiamerl@yahoo.com.br (C. Merlini), guiga@emc.ufsc.br (G.M.O. Barra).

0142-9418/$ – see front matter © 2012 Elsevier Ltd. All rights reserved.
http://dx.doi.org/10.1016/j.polymertesting.2012.07.003

polymer blends depend greatly on the processing conditions, properties of the matrix and disperse phase; and also the characteristics of the conducting polymer, such as particles shape, orientation, aspect ratio and its distribution and dispersion in the polymer matrix [1,4].

Several methods have been used to reduce the percolation threshold and improve the electrical, mechanical and rheological properties in conducting polymer blends. Most published scientific research papers have been employed compatibilizers, such as block copolymers, ionic polymers or functionalized protonic acids inserted into ICP chains, making it possible to form compatible conducting polymer blends at very low conducting polymer content [8–11]. These blends can be normally obtained by mixing both components in solutions or melts [1,4,9,11].

On the other hand, the development of polypyrrole or polyaniline deposited on the fiber surface, such as wool [12], cotton [13], polyester [14], polyamide [15], bacterial cellulose nanofibers [16,17] provide the possibility to combine the tensile strength, light weight and high surface area of fibers with the electrical, optical and magnetic properties of conducting polymers. Moreover, the resulting fiber-conducting polymer can then be incorporated into insulating polymer matrices to produce conducting polymer composites with the lowest conductive filler loading. It is well known that the conductive filler geometry, such as aspect ratio (length-to-diameter), plays an important role in the formation of a conductive network in the insulating polymer matrix. Thus, by increasing the aspect ratio of conductive filler the percolation threshold can be decreased, i. e., lower filler concentration is necessary to ensure physical contact between fibers when compared with sphere particles, as illustrated in Fig. 1.

Based on the above, the focus of this study was to develop a novel polypyrrole-coated amorphous silica short fibers through *in situ* oxidative polymerization of pyrrole (Py) on the surface of natural amorphous silica short fibers (ASF) by using ferric chloride ($FeCl_3$), as an oxidant. The ASF used in this study were produced by processing "spongollite" which is a mineral derived from the skeleton of sponges found in the bottom of lakes and other regions in Brazil [18–21]. Deposits of more than 5 million tons in Brazil have been evaluated, which is an additional motivation for the use of this material [18,19]. The synthesized polypyrrole nanoparticle coated natural amorphous silica short fibers (PPy-ASF) were characterized by Fourier Transform Infrared spectroscopy (FTIR), scanning electron microscopy (SEM) and thermogravimetric analysis (TGA), while electrical conductivity was measured using a four-probe method. PPy-ASF were then blended with polystyrene-block-poly(ethylene-ran-butylene)-block-polystyrene (SEBS) through the solution casting process. The electrical conductivity and percolation threshold values of SEBS/PPy-ASF composites were evaluated and compared with PPy filled SEBS blends.

2. Experimental

Amorphous silica fibers treated with silane agent (Silexil PU), with density of 1.80 g cm^{-3}, were kindly supplied by the Cerâmica São Caetano LTDA. Pyrrole (Aldrich; 98%) was distilled under vacuum and stored in a refrigerator. Iron (III) Chloride Hexahydrate ($FeCl_3 \cdot 6H_2O$) (analytical grade, Vetec) was used without further purification. Polystyrene-block-poly(ethylene-ran-butylene)-block-polystyrene copolymers commercially designated Kraton G1650 was kindly supplied by Kraton Polymers of Brazil. The number of average molecular weight of SEBS G 1650 is 54,000 g mol^{-1} (according to the supplier), with a polystyrene block content of 30 wt.%.

Natural amorphous silica short fibers (ASF) were coated with PPy through *in situ* oxidative polymerization. Firstly, 5 g of ASF were dispersed in 0.125 L of distilled water under stirring at 25 °C, and 0.1 mol·L^{-1} of pyrrole was added. After 10 min, 0.05 mol of iron (III) chloride hexahydratate ($FeCl_3 \cdot 6H_2O$) dissolved in 0.1 L distilled water was slowly added. The polymerization reaction was maintained for at least 4 h. The dark powder was then precipitated in ketone in order to extract the byproducts and dried under vacuum at room temperature. The pure polypyrrole was also synthesized under the same procedure.

SEBS/PPy-ASF composites were prepared through solution casting. Firstly, an appropriate amount of SEBS toluene solution and ASF dispersion were stirred using an ultrasonic probe (50 W and 60 Hz) for 10 minutes. After that, the mixture was cast onto a glass plate to evaporate the solvent at room temperature, resulting in conducting polymer films with thickness lower than 200 μm.

3. Characterization

Attenuated Total Reflectance-Fourier Transform Infrared spectroscopy (ATR-FTIR) was performed in a Bruker spectrometer, model TENSOR 27, in the range of 4000 to 600 cm^{-1} by accumulating 32 scans at a resolution of 4 cm^{-1}.

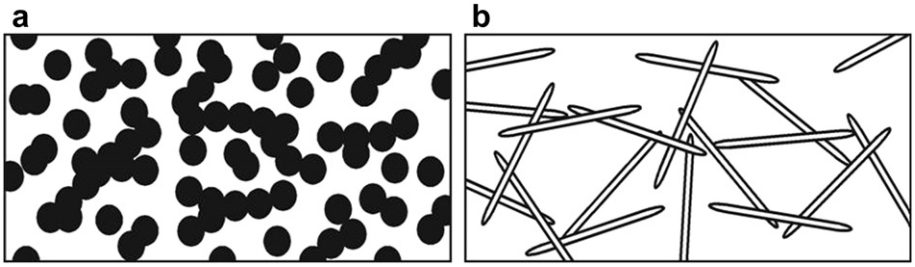

Fig. 1. Illustrative scheme of two hypothetic polymer composites with different conductive fillers geometry: a) spheres and b) fibers (high aspect ratio).

Micrographs of the ASF, PPy-ASF and fractured SEBS/PPy-ASF samples were analyzed by using scanning electron microscopy (SEM), Jeol model JSM-6390LV. ASF and PPy-ASF samples were coated with gold and observed using an applied tension of 10 Kv, while the solution cast specimens were fractured in liquid nitrogen and coated with gold before the cross-section was observed in SEM at an accelerating voltage of 10 kv.

Optical micrographs of the SEBS/PPy-ASF composites and SEBS/PPy blends were analyzed using a Bioval L2000C microscope.

The amount of PPy deposited on silica fibers was determined by thermogravimetric analysis (TGA) using a STA 449 F1 Jupiter® (Netzsch) thermogravimetric analyzer. The analysis was performed at 10 °C min^{-1} from 25 to 700 °C and the nitrogen flow was maintained at 50 cm^3 min^{-1}.

The electrical conductivity of the PPy, PPy-ASF and low-resistivity polymer composites were measured using the four probe standard method with a Keithley 6220 current source to apply the current and a Keithley Model 6517A electrometer to measure the potential difference. For pure SEBS and high-resistivity polymer composites, the measurements were performed using a Keithley 6517A electrometer connected to a Keithley 8009 test fixture. Sample measurements were performed at least five times at room temperature.

4. Results and discussion

The FTIR spectra of ASF, PPy and PPy-ASF are shown in Fig. 2. The absorption bands in the 1050 cm^{-1} and 788 cm^{-1} region for pure ASF refer to the antisymmetric and symmetric Si–O–Si stretching vibrations, respectively [20,21]. The spectrum of PPy exhibits absorption bands at 1540 cm^{-1} and 1458 cm^{-1}, assigned to the C–C and C–N stretching vibration of pyrrole ring, respectively [22]. The broad band at 1290 cm^{-1} is attributed to C–H or C–N in-plane deformation modes while the bands at 1158 and 1030 cm^{-1} are assigned to the C–H bending modes. The FTIR spectrum of PPy-ASF exhibited overlapped absorption bands of both PPy and ASF, indicating that PPy was deposited on the silica fiber surface.

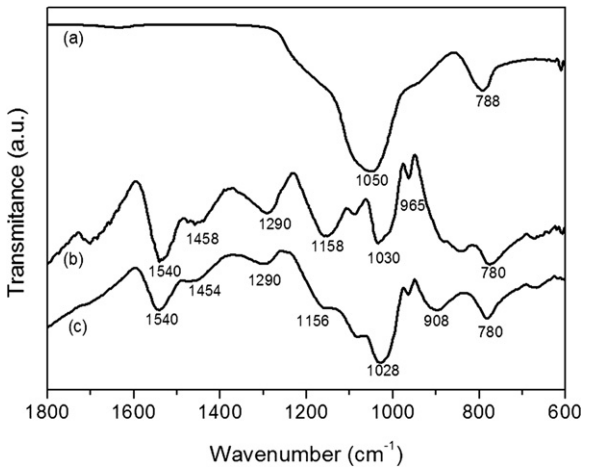

Fig. 2. Infrared spectra of: (a) silica fiber (ASF), (b) polypyrrole (PPy) and (c) PPy-ASF composites.

Scanning electron micrographs of ASF and PPy-ASF surfaces are compared in Fig. 3. As shown in Fig. 3a and b, ASF are tubular and have a central hole with a diameter of about 1 μm, which is related to the space previously occupied by silicatein, an enzyme used by sponges to capture silicate during silica formation [18]. Moreover, ASF exhibit a needle-like shape with one sharp extremity and their surface is smooth. The pure natural amorphous silica fibers show average length of about 451 μm and aspect ratio of about 70 which are higher than found for ASF by Barra et al. [21]. On the other hand, MEV micrographs revealed that PPy-ASF (Fig. 3c and d) were comprised of polypyrrole nanoparticles with a mean size of 50 nm packed close together to form a conducting polymer layer which homogeneously coated the amorphous silica fibers surface. Similar morphology has been observed for silica nanoparticles coated with conducting polyaniline, as reported by Liu et al. [23].

ASF and PPy show electrical conductivity values of 3.00×10^{-10} and 0.53 $S.cm^{-1}$, respectively. The PPy-ASF showed electrical conductivity of 0.32 $S.cm^{-1}$, similar to that found for pure PPy. This result ratifies the formation of the conducting network layer on the ASF surface.

The EDS analysis (Fig. 4) was performed on the ASF surface, where the white layer corresponds to the polypyrrole coated amorphous silica fiber (1) and the black region is the uncoated ASF surface (2). The EDS elementary analysis of uncoated ASF (Table 1) shows that these natural fibers are mainly composed of silicon and oxygen related to the chemical nature of silicon dioxide (SiO_2). Carbon and nitrogen are also observed on the ASF surface due the presence of amino silane coupling agent [22]. The white region related to PPy layer has a considerable amount of carbon and nitrogen with the presence of chloride content, as counter-ion. Iron (Fe) was also observed probably due the presence of oxidant residue.

Fig. 5 shows TGA thermograms of the silica fiber, PPy and PPy-ASF. The silica fibers present a weight loss of 9.15% at 300 °C which is attributed to the dehydration of hydrophilic silica surface [22]. For the pure polypyrrole, the first weight loss starts below 100 °C due the elimination of absorbed water, and above 280 °C corresponds to the polymer chain degradation. The amount of polypyrrole deposited on the silica fibers surface was calculated from TGA curves, comparing the amount of residue of PPy-ASF with those assigned to the ASF and PPy. For this purpose, it was assumed that ASF and PPy in the composite are the origins of an amount of residue proportional to the amount of each pure component. Thus, according to the rule of mixtures, a theoretical relationship for the PPy-ASF was built, considering the amount of residue of pure components and simulating their proportion in the fibers [17]. The PPy deposited ASF surface was about of 17 wt.%.

Fig. 6 shows the variation in the electrical conductivity as a function of PPy for SEBS/PPy-ASF composites prepared through solution casting. As expected, the electrical conductivity increases with increasing amount of PPy in the insulating SEBS matrix due the formation of conducting polymer network. Analogous behavior was observed for

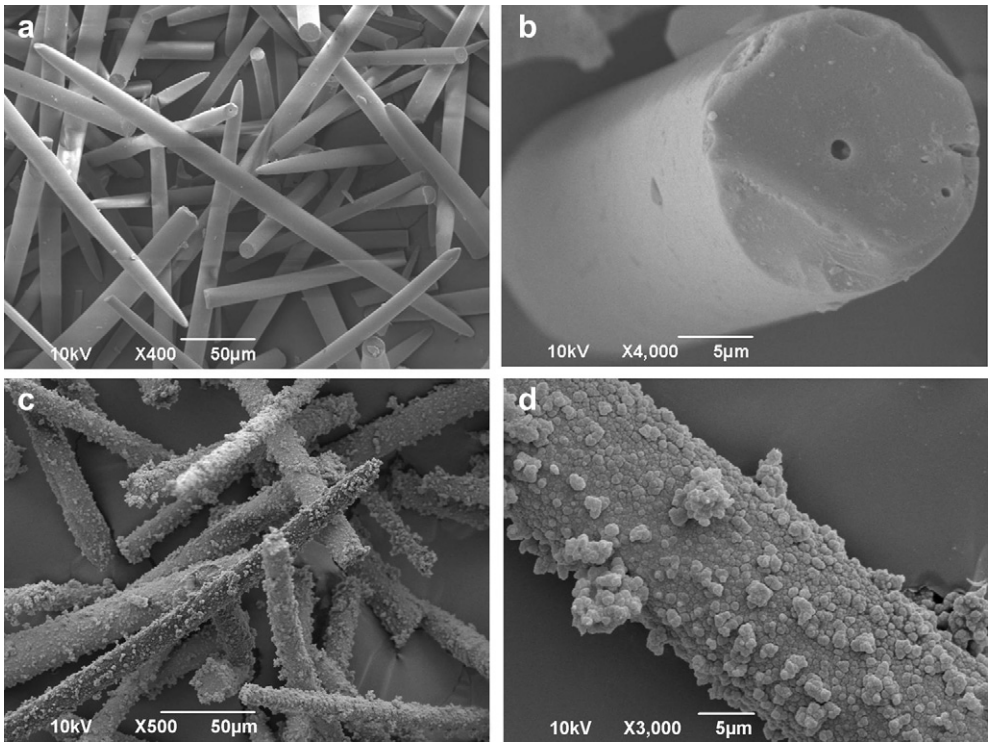

Fig. 3. Scanning electron micrographs of: ASF (a), (b) and PPy-ASF (c), (d).

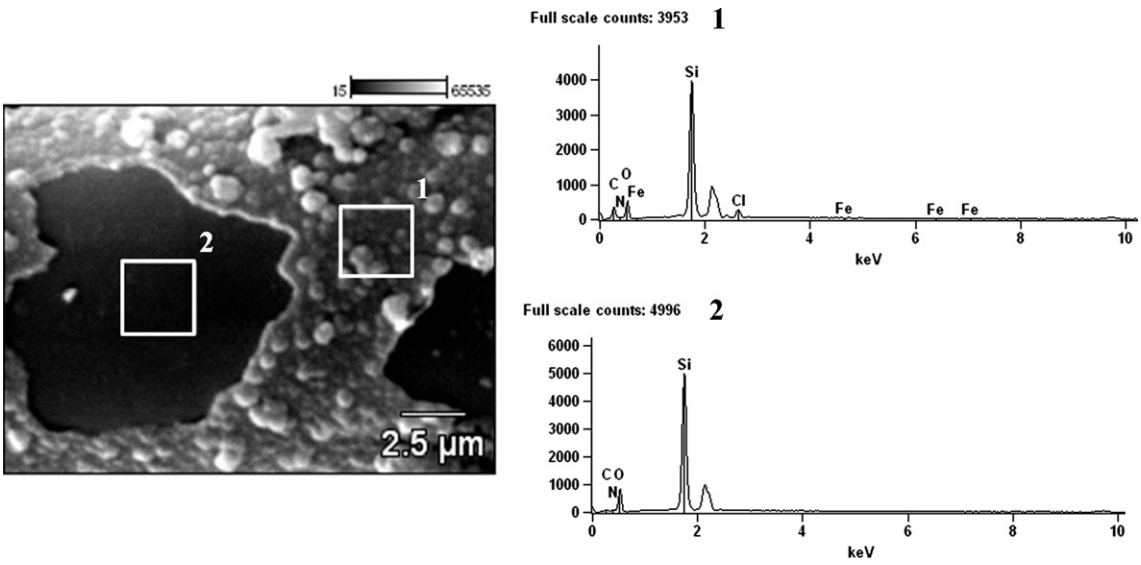

Fig. 4. EDS analysis of PPy-ASF composites (pt1) and silica fiber (pt2).

Table 1
Surface composition of silica fiber and silica coated with PPy (Weight %).

Filler	C	N	O	Si	Cl	Fe
PPy-ASF (1)	40.1 ± 1.5	10.3 ± 2.0	19.2 ± 0.6	27.3 ± 0.2	2.4 ± 0.2	0.7 ± 0.2
ASF (2)	16.5 ± 1.5	4.4 ± 1.6	32.3 ± 0.6	46.8 ± 0.3	–	–

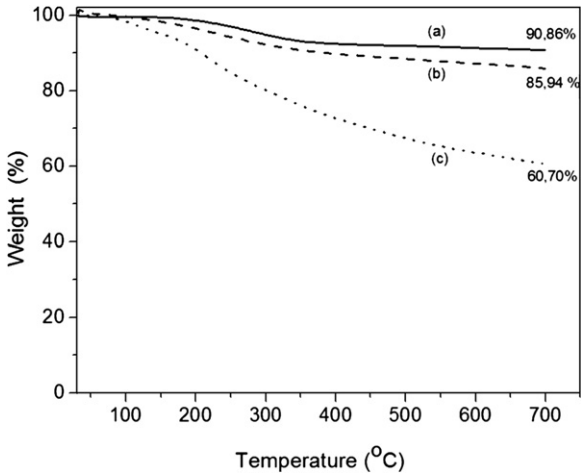

Fig. 5. TGA thermograms of (a) silica fiber, (b) PPy-ASF and (c) PPy.

SEBS/PPy blends prepared under the same conditions. However, SEBS/PPy blends displayed lower electrical conductivity than SEBS/PPy-ASF composites in all compositions studied. For 10 wt.% of conductive filler, the

Table 2
Percolation parameters of PPy-ASF and PPy loaded SEBS mixtures.

Filler	f_p (wt.%)	Critical exponent (t)	Linear correlation coefficient (R)
PPy	6.0	5.1	0.99
PPy-ASF	1.0	6.1	0.97

electrical conductivity of SEBS/PPy-ASF composite was 1.4×10^{-3} S.cm^{-1}, which is about 10^3-fold higher than the value found for the SEBS/PPy blend. For high concentration of PPy, the electrical conductivity for SEBS/PPy blends (75/25) wt.% is still lower than SEBS/PPy-ASF composites (90/10) wt.%. These results are consistent with the morphological features of the composites, as illustrated in Fig. 6. The microstructure of mixtures revealed typical phase separation morphology with the presence of conductive filler (the dark regions seen in the optical micrograph). SEBS/PPy-ASF composites (Fig. 6A) presented disperse fibers comprised of conducting pathways, with the disperse phase better interconnected when compared to the SEBS/PPy blend (Fig. 6B). The microstructure of the SEBS/PPy-ASF composite indicates that the geometry modification of the conductive filler (PPy particles to PPy-

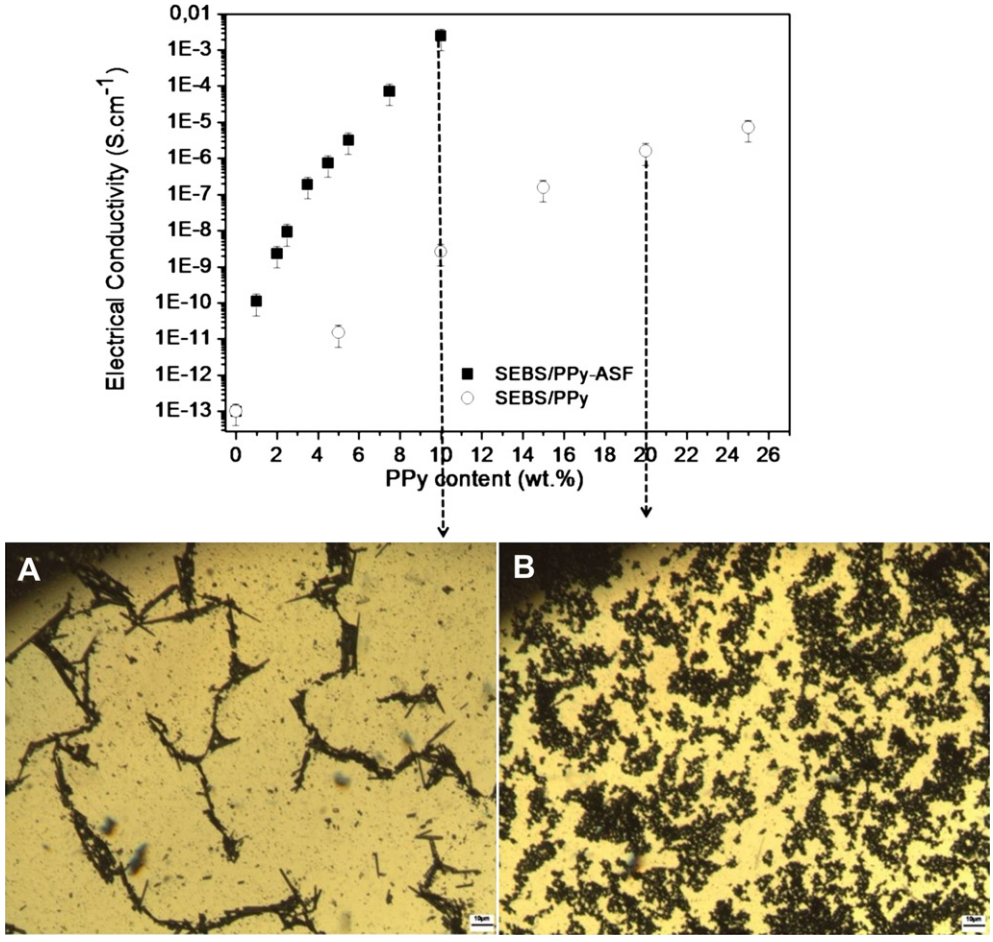

Fig. 6. The effect of conductive filler concentration on the electrical conductivity of SEBS/PPy-ASF composites and SEBS/PPy blends. Optical micrographs of the (A) PPy-ASF (10 wt.%) and (B) PPy (20 wt.%) incorporated into SEBS matrix.

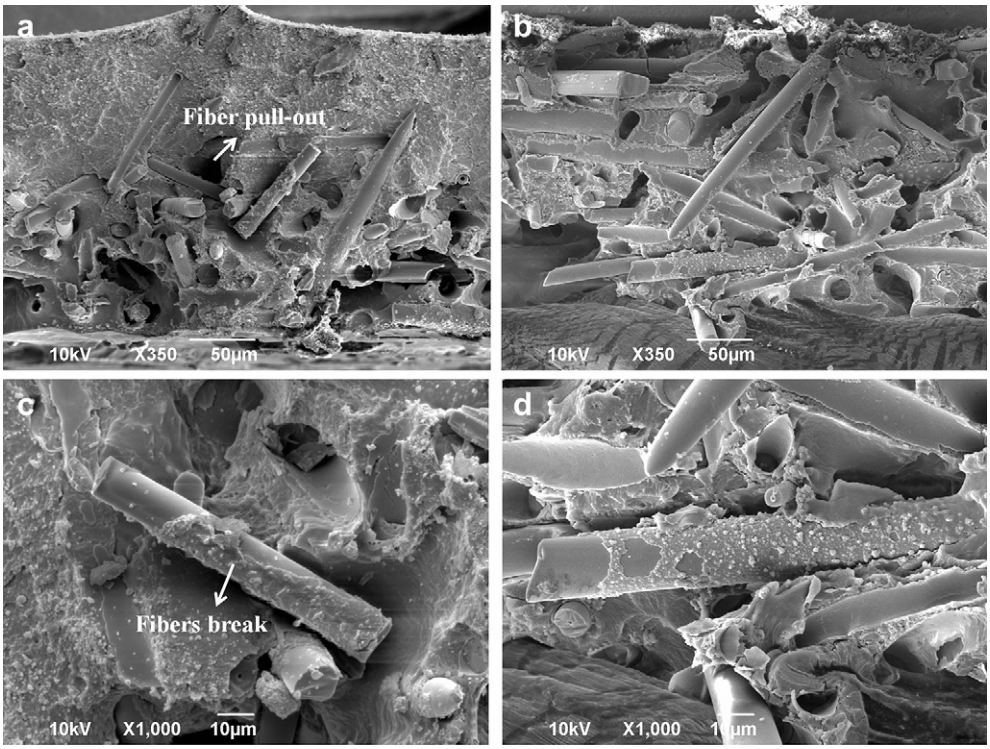

Fig. 7. Scanning electron micrographs of the composites with the matrix SEBS and differents weight fraction of PPy: (a,c) 5 wt.% and (b,d) 10 wt.%.

ASF fibers) was able to improve the formation of the conducting network in the SEBS matrix and, consequently, increase the electrical conductivity values.

The data presented in Fig. 6 was fitted to the scaling law of percolation theory [24], as observed in Eq. (1); in which c is a constant, t a critical exponent, σ_f the conductivity, f the fraction of the conductive medium and f_p the fraction at the percolation threshold, expressed as a weight fraction.

$$\sigma_f = c(f - f_p)^t \quad (1)$$

The percolation threshold (f_p), critical exponent (t) and linear correlation coefficient (R) values calculated by the plot of log σ versus log $(f - f_p)$ are listed in Table 2. The lower f_p value for the SEBS/PPy-ASF composite than SEBS/PPy blend and others reported polymer systems [5,8,10,11] probably reflects the high aspect ratio of PPy-ASF fibers dispersed in the SEBS matrix. Critical exponent values are higher than those predicted from classical percolation theory and can be explained by tunneling-percolation process, as proposed by C. Grimaldi et al. [24].

The effect of the PPy-ASF addition on the morphology of SEBS/PPy-ASF composites was investigated through scanning electron microscopy (SEM). Fig. 7 illustrates the SEM micrographs of cryogenically fractured surfaces of the SEBS/PPy-ASF composites containing 5 and 10 wt.% of the PPy deposited on the amorphous silica fibers surface (Fig. 7a and b), respectively. As observed in Fig. 7, PPy-ASF are uniformly dispersed in the SEBS matrix and the conducting network is evident. In addition, the presence of fiber break and fiber pull out suggests some degree of interaction between PPy-ASF and matrix. A more detailed morphological analysis of SEBS/PPy-ASF composites is shown by high magnification (Fig. 7c and d). The micrographs revealed that the polypyrrole coating was adhered on ASF, and a network comprised of a conducting polymer layer on the fibers surface was responsible for the high electrical conductivity values of the polymer composite.

5. Conclusions

New conducting amorphous silica short fiber coated with conducting polypyrrole was obtained through *in situ* oxidative chemical polymerization of pyrrole. SEM micrographs and FTIR spectroscopy revealed that amorphous silica short fibers (ASF) were successfully coated with PPy. PPy-ASF were comprised of PPy nanoparticles that form an uniform layer on the fiber surface. The amount of PPy deposited on ASF determined by thermogravimetric analysis was about 17 wt.%. Both PPy-ASF and PPy fillers were incorporated separately in the SEBS matrix through solution casting. The geometry of conductive fillers used to prepare conducting polymer mixtures with SEBS strongly affected the electrical conductivity and percolation threshold of SEBS/PPy-ASF composites and SEBS/PPy blends. SEBS/PPy-ASF composites displayed lower percolation threshold and higher electrical conductivity values than those found for PPy filled SEBS blends. Optical analysis revealed that the SEBS/PPy-ASF composites exhibited a conducting phase better interconnected in the SEBS matrix when compared to the SEBS/PPy blends, due the

high aspect ratio of conductive fibers. The results obtained in this study reveal that PPy-ASF materials are promising candidates for developing conducting polymer composites at very low percolation threshold.

Acknowledgements

The authors gratefully acknowledge the financial support by Conselho Nacional de Desenvolvimento Científico e Tecnológico - CNPq, Coordenação de Aperfeiçoamento de Pessoal de Ensino Superior - CAPES, and Fundação de Amparo à Pesquisa e Inovação do Estado de Santa Catarina - FAPESC. We are sincerely thankful to Central Electronic Microscopy Laboratory, Santa Catarina Federal University (LCME-UFSC).

References

[1] S. Bhadra, D. Khastgir, N.K. Singha, J.H. Lee, Progress in preparation, processing and applications of polyaniline, Prog. Polym. Sci. 34 (2009) 783–810.
[2] O.T. Ikkala, T.M. Lindholm, H. Ruohonenc, M. Seläntausb, K. Väkipartack, Phase behavior of polyaniline/dodecyl benzene sulphonic acid mixture, Synth. Met. 69 (1995) 135–136.
[3] L.W. Shacklette, C.C. Han, M.H. Luly, Polyaniline blends in thermoplastics, Synth. Met. 55-57 (1993) 3532–3537.
[4] J. Anand, S. Palaniappan, D.N. Sathyanarayana, Conducting polyaniline blends and composites, Prog. Polym. Sci. 23 (1998) 993–1018.
[5] G.M.O. Barra, R.R. Matins, K.A. Kafer, R. Paniago, C.T. Vasques, A.T.N. Pires, Thermoplastic elastomer/polyaniline blends: evaluation of mechanical and electromechanical properties, Polym. Test. 27 (2008) 886–892.
[6] C. Perruchot, M.M. Chehimi, M. Delamar, J.A. Eccles, T.A. Steele, C.D. Mair, SIMS analysis of conducting polypyrrole–silica gel composites, Synth. Met. 113 (2000) 53–63.
[7] B. Pourabbas, F. Pilati, Polypyrrole grafting onto the surface of pyrrole-modified silica nanoparticles prepared by one-step synthesis, Synth. Met. 160 (2010) 1442–1448.
[8] G.M.O. Barra, L.B. Jacques, R.L. Oréfice, J.R.G. Carneiro, Processing, characterization and properties of conducting polyaniline-sulfonated SEBS block copolymers, Eur. Polym. J. 40 (2004) 2017–2023.
[9] Y. Cao, P. Smith, A.J. Hegger, Counter-ion induced processibility of conducting polyaniline and of conducting polyblends of polyaniline in bulk polymers, Synth. Met. 48 (1992) 91–97.
[10] D.S. Vicentini, G.M.O. Barra, J.R. Bertolino, A.T.N. Pires, Polyaniline/thermoplastic polyurethane blends: preparation and evaluation of electrical conductivity, Eur. Polym. J. 43 (2007) 4565–4572.
[11] D. Müller, M. Garcia, G.V. Salmoria, A.T.N. Pires, R. Paniago, G.M.O. Barra, SEBS/PPy.DBSA blends: preparation and evaluation of electromechanical and dynamic mechanical properties, J. Appl. Polym. Sci. 120 (2011) 351–359.
[12] A. Varesano, C. Tonin, Improving electrical performances of wool textiles: synthesis of conducting polypyrrole on the fiber surface, Text. Res. J. 78 (2008) 1110–1115.
[13] K.F. Babu, R. Senthilkumar, M. Noel, M.A. Kulandainathan, Polypyrrole microstructure deposited by chemical and electrochemical methods on cotton fabrics, Synth. Met. 159 (2009) 1353–1358.
[14] J. Molina, A.I. del Río, J. Bonastre, F. Cases, Chemical and electrochemical polymerization of pyrrole on polyester textiles in presence of phosphotungstic acid, Eur. Polym. J. 45 (2009) 1302–1315.
[15] A. Kaynak, S.S. Najar, R.C. Foitzik, Conducting nylon, cotton and wool yarns by continuous vapor polymerization of pyrrole, Synth. Met. 158 (2008) 1–5.
[16] D. Müller, C.R. Rambo, D.O.S. Recouvreux, L.M. Porto, G.M.O. Barra, Chemical in situ polymerization of polypyrrole on bacterial cellulose nanofibers, Synth. Met. 161 (2011) 106–111.
[17] J.A. Marins, B.G. Soares, K. Dahmouche, S.J.L. Ribeiro, H. Barud, D. Bonemer, Structure and properties of conducting bacterial cellulose-polyaniline nanocomposites, Cellulose 18 (2011) 1285–1294.
[18] H.C. Schröder, A. Krasko, D. Brandt, M. Wiens, M.N. Tahir, W. Tremel, W.E.G. Müller, Silicateins, silicase and spicule-associated proteins: synthesis of demosponge silica skeleton and nanobiotechnological applications, in: Porifera Research: Biodiversity, Innovation and Sustainability (2007), pp. 581–592.
[19] E.N. Gregolin, H. Goldenstein, M.C. Gonçalves, R.G. Santos, Aluminium matrix composites reinforced with co-continuous interlaced phases aluminium-alumina needles, Mater. Res. 5 (3) (2002) 337–342.
[20] C.C. Saliba Jr., R.L. Oréfice, J.R. Carneiro, A. Kasan, W.T. Schneider, M. R.F. Fernandes, Effect of the incorporation of a novel natural inorganic short fiber on the properties of polyurethane composites, Polym. Test. 24 (7) (2005) 819–824.
[21] G.M.O. Barra, M.C. Fredel, H.A. Al-Qureshi, A.W. Taylor, C. Clemenceau Jr., Properties of chemically treated natural amorphous silica fibers as polyurethane reinforcement, Polym. Compos. 27 (2006) 582–590.
[22] M. Omastová, M. Trchová, J. Kovářová, J. Stejskal, Synthesis and structural study of polypyrroles prepared in the presence of surfactants, Synth. Met. 138 (2003) 447–455.
[23] Y.D. Liu, F.F. Fang, H.J. Choi, Silica nanoparticle decorated conducting polyaniline fibers and their electrorheology, Mater. Lett. 64 (2010) 154–156.
[24] C. Grimaldi, T. Maeder, P. Ryser, S. Strässler, Critical behaviour of the piezoresistive response in RuO2–glass composites, J. Phys. D: Appl. Phys. 36 (2003) 1341–1348.